JOURNAL OF MATERIALS SCIENCE 4 (1969) 817–835

Review: Radiography with Neutrons

M. R. HAWKESWORTH, J. WALKER
Department of Physics and Radiation Centre, University of Birmingham, UK

Received 5 May 1969

The use of neutron beams for radiographic purposes is a relatively new method of non-destructive testing. This paper is a general review of the technique. The various sources of neutrons and image recorders which may be used are discussed with particular emphasis on photographic recorders. Problems in which neutron radiography is expected to show advantages over conventional radiography are outlined, and some results are presented.

1. Introduction and Principles

Radiography with gamma-rays and X-rays has been long established as a very important technique of non-destructive testing, but the use of neutrons is only just becoming prominent. Thewlis [1, 2] summarised the early neutron work and Berger [3] has extended the review to 1964 in a monograph which also describes the principles of neutron radiography and gives some examples of its use. Neutrons should not be regarded as competitors to X- and gamma-rays for simple radiography but there are circumstances when their particular characteristics make them a valuable additional tool; these characteristics will be discussed later. The availability of suitable neutron sources and detectors has obviously played an important part in influencing the rate of radiographic applications. The very early work was performed with comparatively weak sources and, understandably, did not give radiographs of very high quality. Neutron beams from nuclear reactors have provided much better results and most of the work so far has used reactor sources. Their limitation is lack of portability and, in consequence, there is a growing interest in small accelerator sources and in radioactive (isotope) sources linked with sensitive detectors.

The main components of a neutron radiographic system are shown in fig. 1.

With X- or γ-radiography the source is usually of small size and the radiation is uncollimated; the source-sample distance is kept large enough and the sample-detector distance small enough to ensure satisfactory resolution. With neutrons, the source is often comparatively large and the radiation must then be collimated to provide the necessary resolution. Fortunately, the neutron sources which are physically large provide neutrons of energies where collimation is straightforward. The detector for neutrons cannot be a simple film because the detection efficiency is too low, but film can be used very effectively with an appropriate *converter* screen to convert the neutrons into photoeffective radiation such as light or charged particles.

Let us assume that the combination of source and collimator provides I_0 neutrons cm^{-2} sec^{-1} approximately normal to the face of the sample which is shown in fig. 1 as having two components of lengths x and x^1 and with effective attenuation coefficients Σ, Σ^1.

On this simple model, the neutron current densities from the two parts of the sample would be:

$$I_1 = I_0 e^{-\Sigma x},$$

$$I_2 = I_0 e^{-(\Sigma x + \Sigma^1 x^1)}.$$

To record the presence of the second component in the target, the radiation intensity I_1 would have to be adequate to operate the detector and the difference between I_1 and I_2 would have to be detectable. This simple model neglects the possible differences introduced by scattering in one part of the sample causing a response in the detector associated with the other; a small collimator between the sample and the detector can reduce this effect. Barton [4] has considered the effect of scattered radiation on the contrast of radiographs.

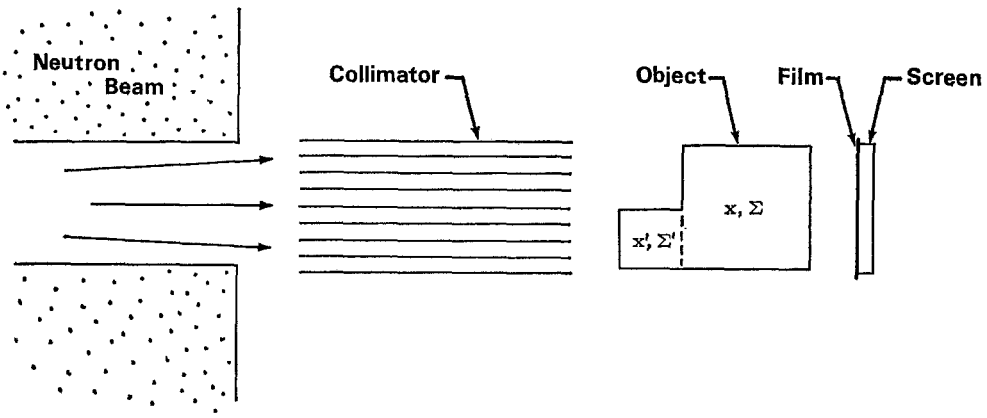

Figure 1 A schematic drawing of the equipment for neutron radiography.

If the detector has a linear response to I_1 and I_2, the fractional change in recorded beam strength is

$$\frac{I_1 - I_2}{I_1} = 1 - e^{-\Sigma^1 x^1} \simeq \Sigma^1 x^1$$

for thin defects. A combination of X-ray film with a converter plate in which β-particles are produced by neutron-induced radioactivity gives a linear relationship ($D = GE$) between image density, D, and exposure, E (neutrons cm^{-2}). In this case the fractional change in image density will be

$$\frac{D_1 - D_2}{D_1} = \Sigma^1 x^1 .$$

(Density is used here in the usual photographic sense; $D = \log A_0/A_1$ where A_0 is the response of a linear photometer without the image in the test beam and A_1 is the response with it.)

If the minimum detectable change in density is $\Delta D_{\min}$, then the minimum detectable change in object thickness is $\Delta D_{\min}/GE\ \Sigma^1$. More sensitive (faster) photographic detectors, those using light emitting screens, have a logarithmic response rather than a linear one; they are discussed in section 4.1.5.

2. Special Features of Neutron Radiography

Neutrons are uncharged and their interaction with matter is therefore only through nuclear forces; the extra-nuclear electrons play no direct part. The action of the neutron's magnetic moment can also be completely neglected in radiography. The neutron-nucleus interaction can involve scattering, elastic (n, n) or inelastic (n, n^1), or absorption in reactions such as radiative capture (n, γ) or those, such as (n, α), with charged particle emission. The nature and the chance of an interaction depend on the energy of the neutron and the structure of the nuclide concerned, not on its charge; this last point is in contradistinction to the situation with X- and γ-rays where only the charge is important.

The prominent fundamental consequences of the neutron interactions and their impact on radiographic applications are:

(i) The cross-section can vary markedly from nuclide to nuclide even with the same element and it is possible to distinguish not only between materials of similar atomic number but also between isotopes. Radiographic searches can therefore be made for particular isotopes if their cross-sections are high enough (figs. 2 and 3). Fig. 4 illustrates the comparative situation for 125 keV X-rays and 0.025 eV neutrons (this is the energy of a neutron with the modal speed of the Maxwell-Boltzmann distribution at 20° C). The attenuation coefficient used as the ordinate is more familiar to neutron physicists as the macroscopic cross-section ($\Sigma = N\sigma$), the product of the number of nuclei per cm^3 and their total microscopic cross-section. It is clear that the gradual increase of attenuation coefficient with atomic number shown for X-rays is not present for thermal neutrons and it is therefore possible for neutrons to give radiographs through considerable thicknesses of certain heavy materials, such as lead, where the attenuation coefficient is small. Moreover, radiographs can be obtained of very light elements behind considerable thicknesses of heavy ones; a striking combination is that of hydrogen and lead.

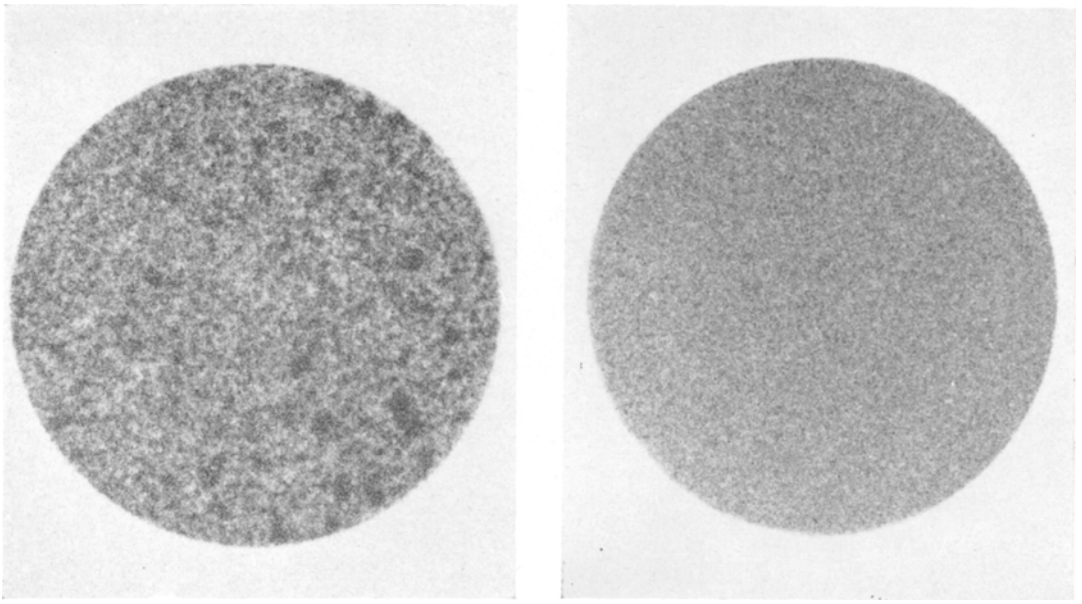

Figure 2 Neutron radiographs of a prototype material for nuclear reactor control elements–a gadolinia-magnesia compact (actual diameter 6 mm). In this instance the test was for adequate mixing of the powders, but later, during irradiation, it could be to assay for ^{155}Gd and ^{157}Gd – highly neutron absorbing isotopes of gadolinium which are converted during service to ^{156}Gd and ^{158}Gd – isotopes with low neutron absorption.

The radiographs were obtained on Ilford HP3 film using a 25 μm gadolinium foil screen behind the film and an exposure of 1.6×10^8 thermal neutrons per cm^2.

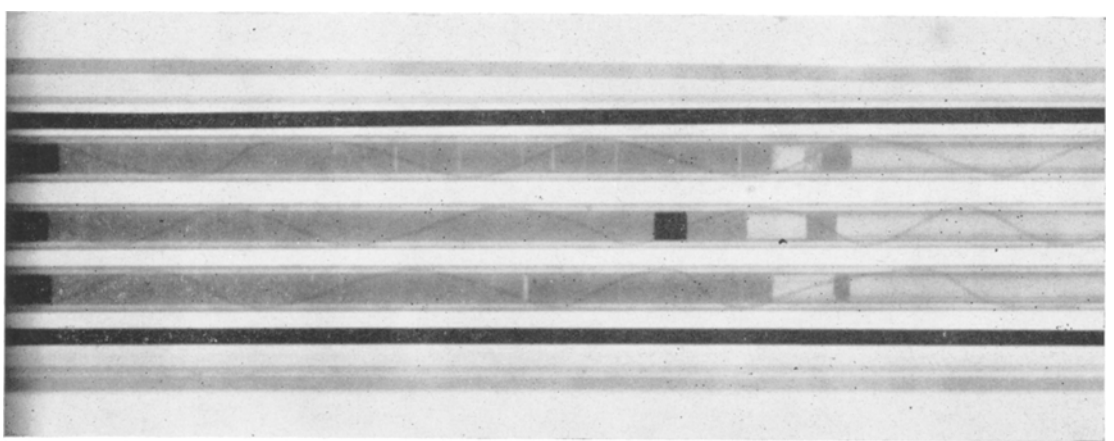

Figure 3 A neutron radiograph of a fast reactor fuel element (actual overall diameter about 7 cm) tested for the correct positioning of the fuel pellets, some of which contain natural uranium (mainly ^{238}U) and others uranium enriched in the more highly neutron-absorbent isotope ^{235}U. The radiograph clearly shows a misplaced ^{235}U pellet. (Reproduced by courtesy of J. P. Barton, Argonne National Laboratory, USA.)

Hydrogenous materials such as water or plastics (figs. 5 and 6) give high scattering of neutrons because the scattering of neutrons by free protons, already high, is increased by a factor of approximately four for slow neutrons when the proton is bound in a heavy molecule. Other light elements such as boron and lithium have high absorption cross-sections and, again, can be

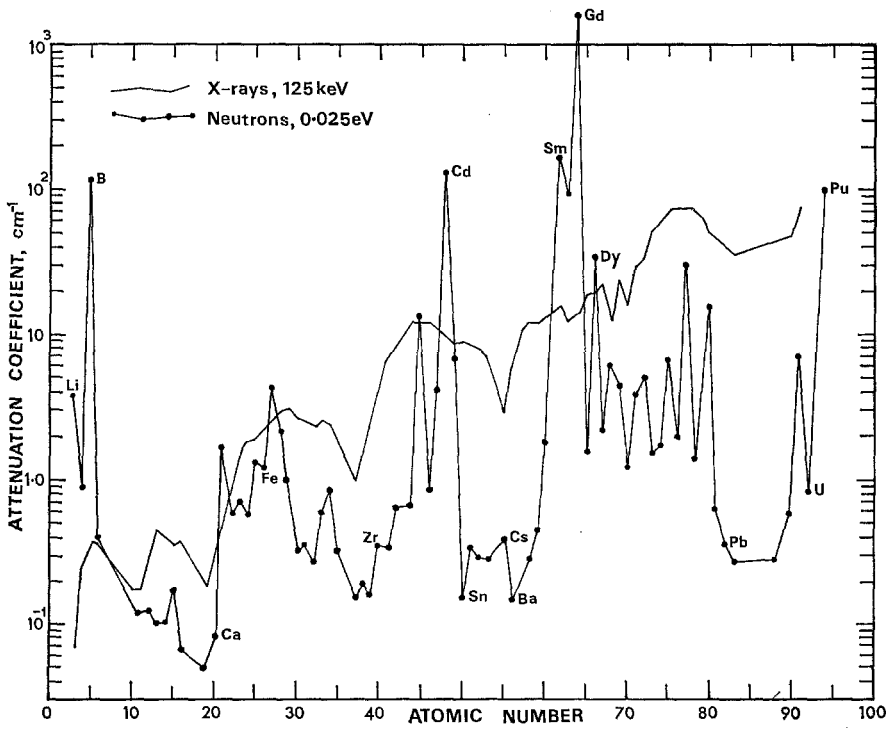

Figure 4 The variation of total attenuation coefficients with atomic number for the solid elements demonstrating the difference between coefficients for X-rays of energy 125 keV and thermal neutrons.

detected easily even when screened by heavy elements. Boron and, at higher masses, cadmium and gadolinium indicate the obvious value of neutron radiography in nuclear reactor technology (fig. 7); these elements and others, very suitable for radiography because of their high neutron absorption, are, for the same reason, important in reactors. Neutron radiography may be used to check their distribution when they are wanted, as in control rods, or their absence when they are not, as in fuel elements.

(ii) The cross-section of a nuclide for neutrons can vary markedly from one neutron energy to another because of resonances in the neutron-nucleus interaction. Fig. 8 gives the examples of cadmium and indium over quite a narrow range of neutron energies. It is clear that a beam of thermal neutrons can be used for the radiography of cadmium objects shielded by other materials, including indium, whereas neutrons of 1.4 eV energy will indicate indium when shielded by other materials including cadmium. A very limited amount of information on neutron-nucleus resonances* is given in table I which also includes cross-sections for neutrons of thermal energies (0.025 eV with a speed of 2200 m sec^{-1}) and at energies of 2.6, 10 and 14 MeV. These last energies are those of the neutrons emitted by the most popular accelerator sources (see section 3). The fast neutron data are included to show that the variations of cross-sections from one element to another are considerably less than for thermal neutrons. An example of the variation of cross-section with energy for very low energies (cold neutrons) is shown in fig. 9 for the case of neutron scattering by iron. The very rapid fall at energies below approximately 0.005 eV arises because the equivalent neutron wavelengths (> 4 Å) are too long for Bragg scattering to occur. This means that neutrons of these energies will have a low removal coefficient and can be used for radiography through considerable thicknesses of iron and steel, both because the transmitted beam intensity is high and because the low scattering maintains good contrast. In this laboratory, Barton [5] has radiographed thin polythene samples behind steel sheet and has

*Details can be obtained from the Brookhaven National Laboratory compilation BNL 325.

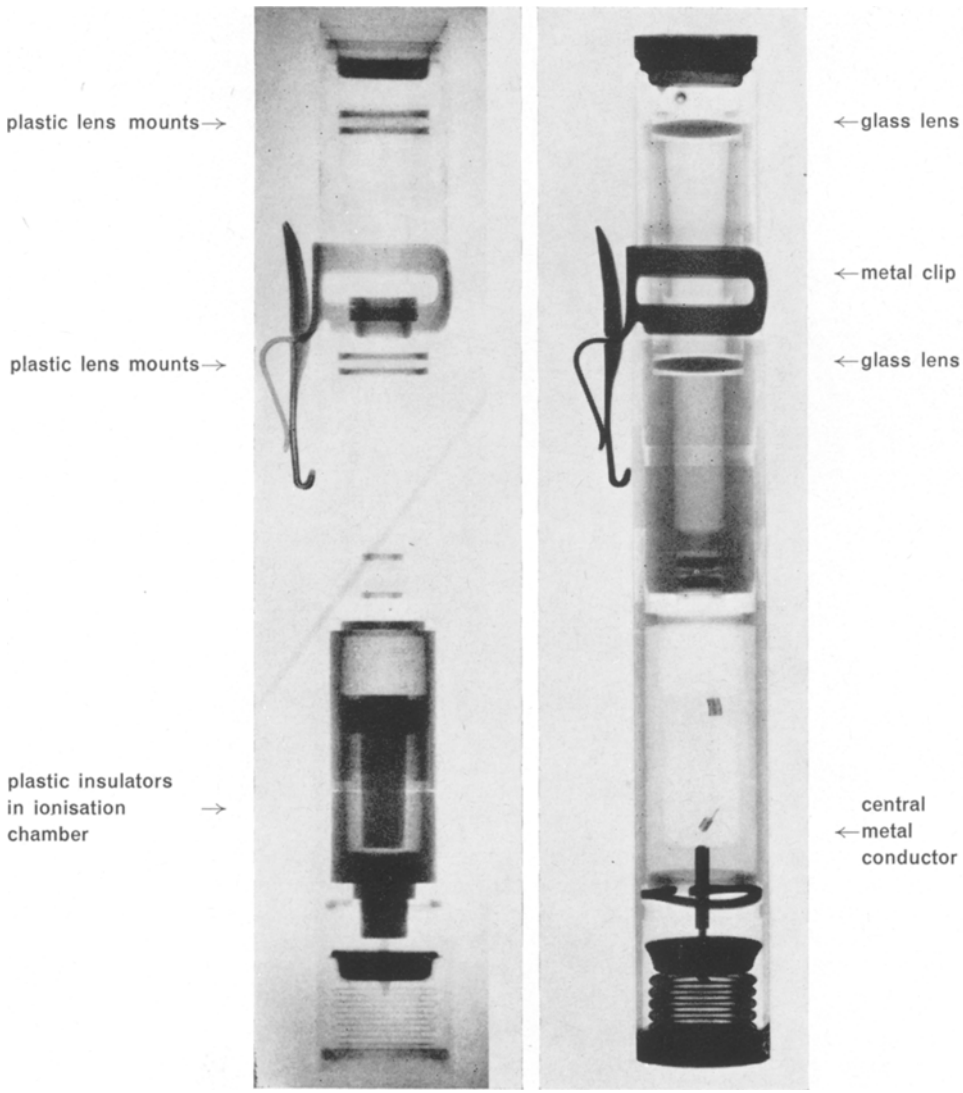

Figure 5 A neutron radiograph (left) and an X-radiograph of a pocket dosemeter – a good illustration of the complementary nature of the two techniques – each showing detail the other has difficulty in revealing. The neutron radiograph is a good example of the use of neutrons for the testing of light materials since any malforming of the ionisation chamber would show clearly. Light (organic) materials are in increasing use in industry particularly in aero-space projects. Suitable radiographic examples are the testing for the correct positioning of O-ring seals and the forming of explosive bolts.

The neutron radiograph was obtained on Ilford Industrial G film using a 25 μm gadolinium screen behind the film and an exposure of 10^8 thermal neutrons per cm^2. The X-radiograph was also obtained on Industrial G film with no screen and an exposure of 36 mAs (ffd 30cm)at 80 kVp.

shown that there is little loss in contrast up to the maximum thickness used, 10 cm.

(iii) Neutron radiography can be used when the samples are highly radioactive and emitting radiations which would preclude X- or γ-radiography. For such an application the converter foil is activated on its own and then placed on the recording film away from the neutron irradiation region. Thermal neutrons are again very suitable for this *transfer technique* because they are potent agents for inducing radioactivity of a convenient lifetime in a

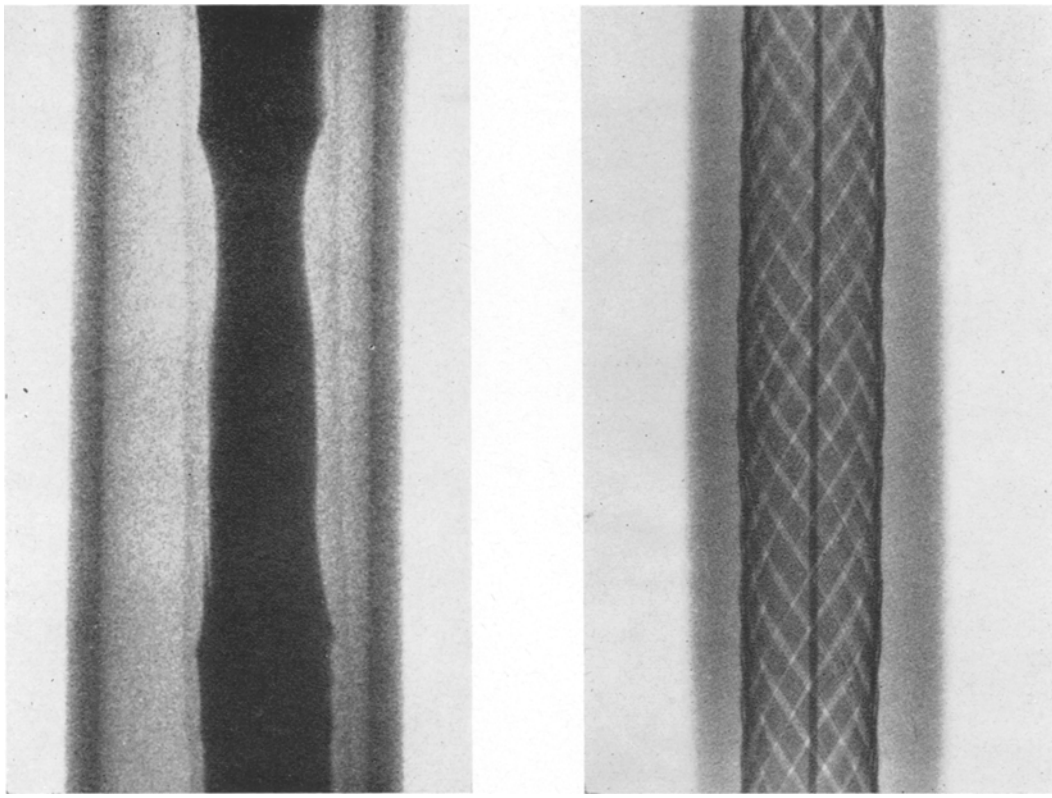

Figure 6 A neutron radiograph (left) and an X-radiograph of a coaxial cable with defective insulation in 2 cm steel conduit (wall thickness 2 mm) – an example of the ability of neutrons to reveal light materials behind heavy ones.

The neutron radiograph was obtained on Ilford Industrial G film using a 25 μm gadolinium screen behind the film and an exposure of 7×10^7 thermal neutrons per cm^2. The X-radiograph was obtained on Industrial G film also, but no screen was used and the exposure was 144 mAs (ffd 30cm) at 80 kVp.

converter; examples of activation are given in the section on detectors. Barton and Perves [6] have given an example of a neutron radiograph of a 10 000 curie uranium sample (fig. 10). It is interesting to note that the transfer technique can be used to overcome other environmental difficulties such as those associated with very high temperatures.

3. Neutron Sources

Nuclear reactors, accelerators and radioactive materials can all be used to provide neutrons through appropriate nuclear reactions. In reactors, nuclear fission is the source reaction. With accelerators, a number of possibilities exist including the bombardment of deuterium, tritium or beryllium by deuterons D(d, n)^{3}He, T(d, n)^{4}He or ^{9}Be(d, n)^{10}B, or the bombardment of lithium or tritium by protons ^{7}Li(p, n)^{7}Be or T(p, n)^{3}He. The T(d, n) reaction is particularly important for low-energy accelerators because the resonance in the cross-section at a deuteron energy of 120 keV results in a high yield of neutrons for accelerating potentials in the region of 100 kV to 500 kV. Accelerators for these energies are comparatively economical to construct. The reactions ^{9}Be(α, n)^{12}C and ^{9}Be(γ, n)^{8}Be(^{4}He) are valuable for use with the α- and γ-radiations from radioactive materials such as radium, plutonium, polonium, americium and antimony. ^{241}Am–Be is now probably the most commonly used (α, n) source of this type; it has a long half-life (458 y), gives about 2.5×10^6 neutrons/sec for 1 curie of ^{241}Am and the associated gamma-radiation of energy 60keV (2.5 mR/h at 1 m for 1 curie), is easily shielded without significant loss of neutrons. A higher yield at the expense of lifetime can be obtained

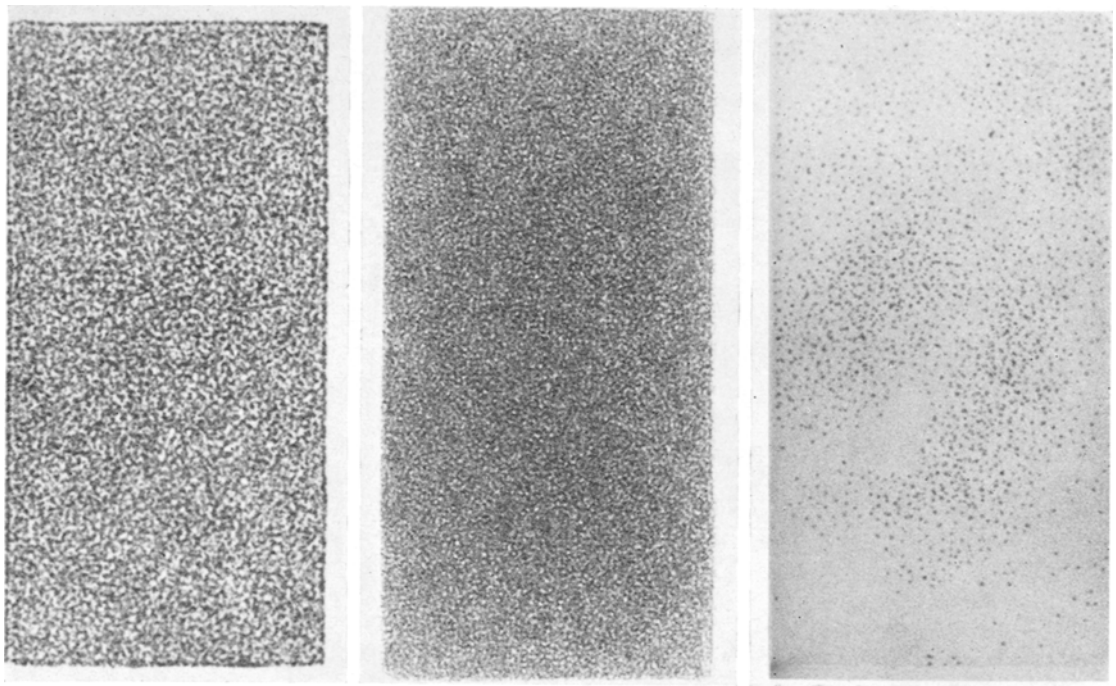

Figure 7 Neutron radiographs and a X-radiograph (centre), of a prototype material for reactor control elements – a boron carbide-stainless steel cermet (actual sample size 2.4 × 1.2 cm). The test was to illustrate the distribution of the boron carbide particles (mean diameter 100 μm); both good and bad mixing are shown. In this particular case X-rays can also illustrate the boron carbide distribution but this would not be possible during service when the control element would be radioactive or if the matrix had been aluminium rather than stainless-steel. Note the positive-negative relationship between the X-radiograph and the left-hand neutron radiograph.

The neutron radiographs were obtained on Ilford HP3 film using a 25 μm gadolinium screen behind the film and an exposure of 3×10^8 thermal neutrons per cm^2. The X-radiograph was obtained on Ilford Industrial G film with no screen at an exposure of 120 mAs (ffd 30cm) at 80 kVp.

by irradiating the ^{241}Am–Be source in the neutron flux of a nuclear reactor which converts ^{241}Am into ^{242}Cm by neutron capture and β-decay, and hence forms a mixed source, ^{241}Am– ^{242}Cm–Be. The half-life of ^{242}Cm is 163 days and the effective specific activity of the source can therefore be increased considerably from its value for ^{241}Am alone; a factor of about 100 has been obtained. For work not requiring a long life-time, the economical ^{124}Sb–Be source, of the (γ, n) type, may also be considered. Its half-life is 60 days and it gives 1.3×10^6 neutrons/sec for 1 curie, but the gamma dose rate is high (1 R/h at 1 m). Spontaneous fission in californium (^{252}Cf) is likely to become an increasingly important source of neutrons as the amount of material available from high-flux reactors increases; the yield is 2.6×10^{12} n/sec g.

Details on these various sources are already available [3, 7–9] and the intention here is to present only those features of special interest in radiography. The first point of note is that all the source reactions give neutrons with energies considerably higher than those required for the majority of radiographic applications. Fission neutrons, for example, have an average energy of about 2 MeV and those from the T(d, n) reaction have an energy of 15 MeV in the forward direction relative to the deuteron beam and 13.2 MeV in the backward direction, for a deuteron energy of 0.2 MeV; energies of a few keV can be produced in low-yield reactions involving medium-weight nuclei. Slow neutrons, however, have to be produced by slowing down the primary ones in a suitable moderator. For radiographic work this will be, almost certainly, ordinary water, a lubricating oil, or a hydrogenous solid. Nuclear reactors which are likely to be

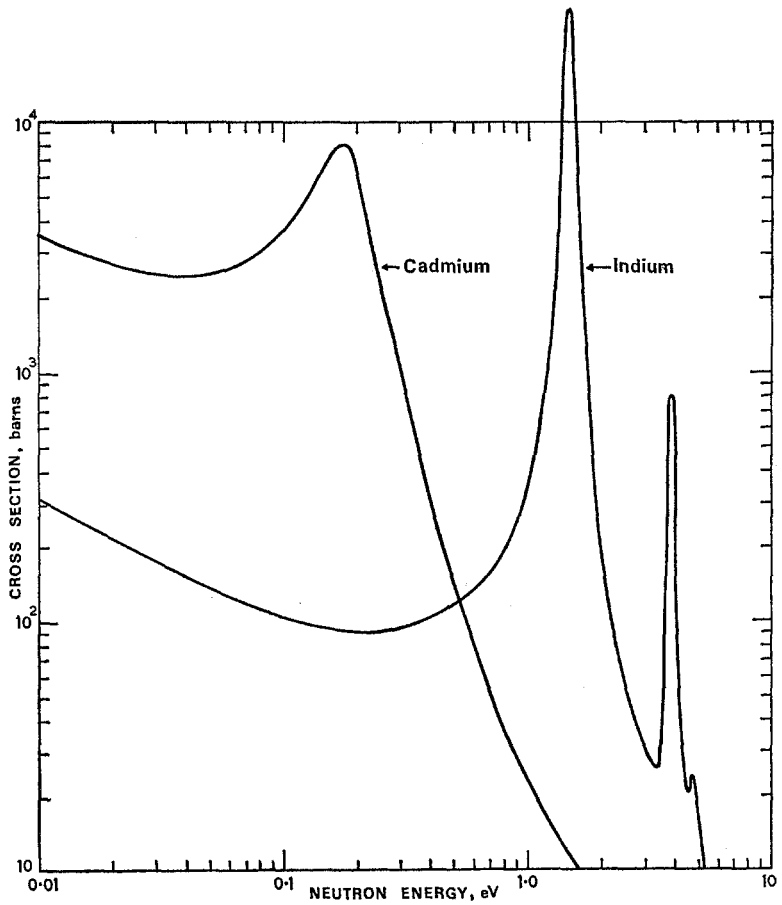

Figure 8 Variation of the total cross-sections of cadmium and indium with neutron energy.

used for radiography (thermal reactors) need an internal moderator in any case, to maintain the fission chain reaction and often have an extra moderator (the thermal column) outside the core to provide a region of well thermalised neutrons free from fast neutron contamination. Once a moderator is present the effective source of neutrons is broad and some form of collimation is necessary to obtain high resolution radiographs. With reactors, adequate collimation is often given by the beam hole through the concrete biological shield but further improvement can be obtained by an additional multi-slit (Soller) collimator formed from plates of cadmium or other thermal neutron absorber and placed in the beam hole or just outside it. For radiography with a pool reactor, Barton and Perves [6] have used a simple conical collimator in the water moderator. A good estimate of the rate at which neutrons emerge from a beam tube with a constant scalar flux ϕ n cm^{-2} sec^{-1} at its inner face is given by diffusion theory as:

$$\frac{AA^1}{4\pi R^2}\left(\phi + \frac{1}{\Sigma}\frac{\partial\phi}{\partial z}\right), \qquad (1)$$

where A, A^1 are the areas of the inner and outer faces of the tube, R is its length (taken to be in the z direction) and Σ is the macroscopic total cross-section of the moderator at the inner face.

The flux gradient $(\partial\phi/\partial z)$ at the inner face is usually small and hence

$$\text{Emerging neutrons per sec} \simeq \frac{AA^1}{4\pi R^2}\phi\,.$$

The beam intensity will obviously depend on the degree of collimation; fig. 11 shows the ratio of the number of neutrons emerging per unit area per second (neutron current) to the scalar flux at the inner face as a function of the beam divergence for a simple cylindrical beam hole.

TABLE I Total microscopic cross-sections of some materials at various energies of interest in neutron radiography

Material	0.005 eV	0.025 eV	Resonances (energy in brackets)		2.6 MeV	10 MeV	14 MeV
Water	165	103	none	none	42	41	41
Lithium	160	72	11 (260 keV)	none	1.9	1.6	1.4
Magnesium	~ 3	3.5	8.4 (20 keV)	46 (84 keV)	3.0	1.6	1.7
Aluminium	3	1.6	53 (5.9 keV)	35 (35 keV)	3.2	1.7	1.7
Calcium	7.5	3.4	6.4 (88 keV)	20 (130 keV)	3.5	2.5	2.2
Manganese	40	16	3300 (400 eV)	950 (1.1 keV)	3.6	3.0	2.6
Iron	7	14	6700 (1.1 keV)	85 (26 keV)	3.3	3.1	2.6
Cobalt	100	45	6800 (135 eV)	320 (4.3 keV)	3.4	3.2	2.7
Copper	12	11	330 580 eV	300 2.1 keV	3.2	3.5	2.9
Zinc	~ 5	5.2	330 (505 eV)	490 (2.6 keV)	3.3	3.5	2.9
Zirconium	6.2	8.2	380 (292 keV)	75 (676 eV)	4.3	4.3	3.9
Silver	140	69	12 500 (5.2 eV)	800 (16.6 eV)	4.8	4.5	4.3
Cadmium	5000	2475	7800 (0.175 eV)	130 (28 eV)	4.8	4.5	4.5
Indium	430	193	29 000 (1.45 eV)	900 (3.9 eV)	5.0	4.5	4.5
Gadolinium	92 000	50 000	310 (2.05 eV)	1300 (2.6 eV)	6.5	5.1	5.2
Dysprosium	2600	1057	1050 (1.75 eV)	7400 (5.5 eV)	6.6	5.2	5.2
Iridium	960	440	4700 (0.65 eV)	5500 (1.3 eV)	7.0	4.9	5.2
Gold	220	98.8	30 000 (4.9 eV)	1000 (60 eV)	7.2	5.0	5.3
Lead	2.6	11	10.7 (350 keV)	8.1 (520 keV)	7.0	5.1	5.3
Uranium	25	16	4200 (6.6 eV)	2200 (21 eV)	7.6	5.6	5.7

Notes: 1. All values have been extracted from "Neutron Cross Sections" by D. J. Hughes and R. B. Schwartz (USAEC, 1962). In general the two resonances with lowest energy have been quoted but occasionally a minor resonance of lower energy has been neglected. All cross-sections are in barns (1 barn $\equiv 10^{-24}$ cm^2).
2. The choice of 0.005 eV as a representative "cold" neutron energy is somewhat arbitrary. It is the energy of the "Bragg cut-off" for iron. The cut-off energy varies, of course, with the element.

Some indications of the neutron fluxes available in nuclear reactors have been given by Walker [9] and can be used to estimate the neutron currents from relation 1 or fig. 11; the fluxes range from 10^{11}n/cm^2 sec for a small research reactor to about 10^{15}n/cm^2 sec in the latest high-flux research reactor. For radiography the low-flux systems are still valuable. A guide to the thermal neutron fluxes which can be produced by accelerator and isotope sources is given in table II. Much more powerful accelerator sources than those quoted are available but are unlikely to be built solely for radiography. The relative merits of reactor, accelerator and isotope sources are as follows. A reactor, if available, is a very suitable source because of its intensity but it is obviously not portable. A low-voltage accelerator is comparatively economical, although

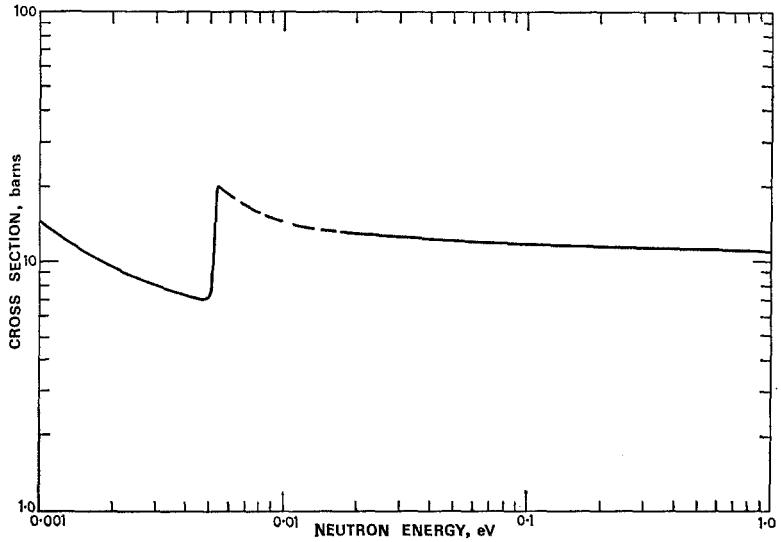

Figure 9 Variation of the total cross-section of iron with neutron energy.

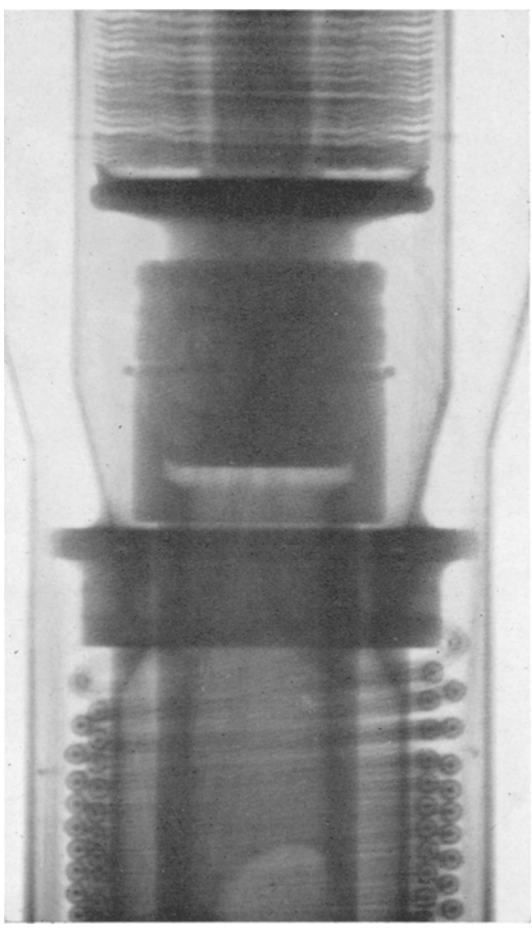

Figure 10 A neutron radiograph of a radioactive fuel test rig (diameter of heated section about 3 cm) – a test during service to locate a fault in the heating circuit. (Reproduced by courtesy of J. P. Perves, Centre D'Etudes Nucleaires de Grenoble.)

The transfer technique was used with a 100 μm indium foil being exposed to 9×10^9 thermal neutrons per cm^2 in 5 min. and then pressed against Kodak Type M film for 30 min.

Similar tasks of this kind for which neutron radiography has been used are the metrology of fuel specimens during irradiation and the reading of melt-wire temperature gauges.

the cost of targets should not be overlooked, and the smaller versions are portable if power supplies are available; it gives a reasonably high yield and can give a range of precise neutron energies which may become useful for some materials. An isotope source is the simplest to use and is easily portable if the shielding required is not too heavy; at the present time only comparatively weak sources can be obtained but the greater availability of ^{252}Cf will alter this situation.

The use of very low energy ("cold") neutrons has been mentioned earlier. A beam of them is obtained from a reactor by filtering a thermal neutron beam with a polycrystal of beryllium, typically 20 cm long, 10 cm diameter, cooled by liquid nitrogen. Neutrons with energies above

about 5 meV (wavelengths less than 4 Å) are scattered out of the beam but low-energy neutrons suffer very little scattering and are transmitted. The intensity of the cold neutrons can be enhanced by having a vessel with liquid hydrogen or liquid deuterium as part of the moderator at the inner face of the beam tube [9].

A guide to the likely neutron beam intensities from the various sources is given in table III. In this table the entry "reactor monochromator" refers to the use of a crystal spectrometer to select neutron energies.

TABLE II Thermal neutron fluxes at the centre of the common source–moderator assemblies*

Source, strength	Half-life cost	Moderator sphere radius† and centre flux H_2O	D_2O	C	Be	BeO	Diphenyl
Am–Be	458y	20	95	95	50	50	30
1.25×10^7	£1275	6.9×10^4	10^5	1.5×10^4	3.0×10^4	4.4×10^4	9.6×10^3
Cm–Be	163d	20	95	95	50	50	30
1.2×10^8	£1650	6.6×10^5	9.7×10^5	1.5×10^5	2.9×10^5	4.3×10^5	9.2×10^4
Po–Be	138d	20	95	95	50	50	30
1.2×10^8	£1650	6.6×10^5	9.7×10^5	1.5×10^5	2.9×10^5	4.3×10^5	9.2×10^4
Sb–Be	60d	10	75	70	35	40	10
$5.2. \times 10^7$	£322	1.6×10^6	6.3×10^5	1.3×10^5	3.7×10^5	3.3×10^5	8.4×10^4
Th–Be	1.91y	20	95	95	50	50	30
10^8	£2500	5.5×10^5	8.1×10^5	1.2×10^5	2.4×10^5	3.6×10^5	7.7×10^4
^{252}Cf	2.65y	30	110	50	24	24	15
10^9	£1000‡	1.4×10^7	4×10^6	1.4×10^6	4.3×10^6	5×10^6	10^6
D(d, n)^3 He	§	15	110	90	45	50	20
10^{10}		4.8×10^7	3.8×10^7	1.3×10^7	3.6×10^7	5.3×10^7	2.9×10^7
T(d, n)^4 He	§	30	115	130	70	55	55
10^{11}		4.9×10^7	5.4×10^8	4.2×10^7	7.0×10^7	2.8×10^8	1.4×10^8

*Calculated by L. Holland of the University of Birmingham, using Fermi-Age theory, which gives reasonably accurate predictions for all but the hydrogenous moderators for which the figures are for guidance only.
†The sphere quoted is that which gives a flux of 90% of that predicted for an infinite sphere of the same moderator.
‡From the highest figure given by Reinig [24].
§Prices from around £4000 – see manufacturers' publications for details.
Notes: 1. Yields quoted for the isotope sources are the maximum commercially available from the UK [25], with the exception of Cf which is not yet commercially available anywhere. The yields given for accelerators are for likely installations.
2. Units used are; source strength – neutrons/sec, sphere radius – cm, neutron flux – neutrons/cm^2 sec.

TABLE III Beam intensities from the common neutron sources

Source*	Typical useful beam intensity† neutrons/cm^2 sec	Typical beam diameter (max) cm	Comments
Reactor – core moderator	10^7–10^9	20	excellent collimation possible; high γ content
Reactor – thermal column	10^5–10^6	30	excellent collimation possible
Reactor – monochromator	10^4–10^5	3 × 10 (rectangular)	very powerful technique
Reactor – Be filter	10^4–10^6	20	for thick steel objects
Accelerator/moderator assembly	10^3–10^5	10	comparable with reactor sources now, will improve
Am–Be/moderator assembly	10–10^2	10	main hope for field use; still developing

*All provide "thermal" neutron beams (mean energy $\sim$ 0.025 eV) except for the crystal monochromator (beam energies from 0.03 to 3 eV) and the cooled beryllium filter (energies $<$ 0.005 eV).
†Beam intensity is strongly dependent on the degree of collimation used. For the reactor beams the higher figure is typical of reactors with a peak thermal flux of 10^{13} neutrons/cm^2 sec; higher fluxes are available.

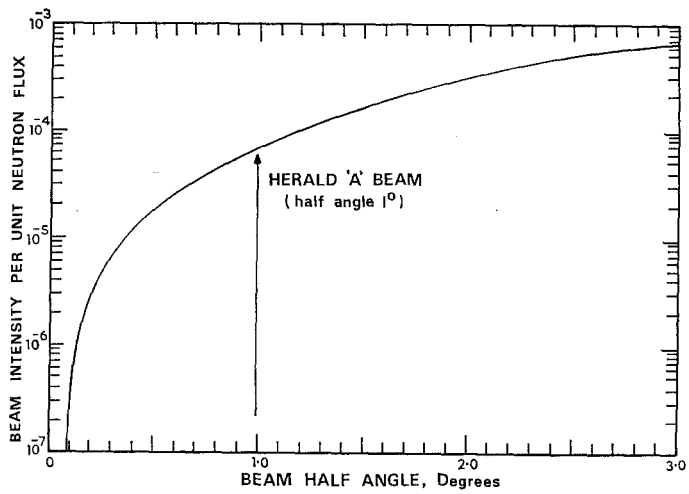

Figure 11 The relation between radiographic beam intensity and the quality of collimation. The "A1" beam from the Herald reactor at AWRE, Aldermaston, was used to obtain the neutron radiographs of figs. 2, 5, 6 and 7.

4. Image Recorders for Neutron Radiography

4.1. Photographic Image Recorders

The most popular image recorder in n-radiography, as in X-radiography, is the photographic emulsion. It offers excellent spatial resolution, a permanent record and the possibility of long recording times in weak neutron fields with simplicity and low cost. Neutrons have insufficient direct effect on photographic emulsions and a converter (intensifier) screen is required to facilitate detection; it is used in the same way as calcium tungstate and lead foil screens in X-radiography. Any material which emits ionising radiation or light following neutron absorption and has the necessary mechanical properties may be used as a screen. There are, of course, many such materials so only the most useful will be mentioned here. These fall logically into the three categories: granular or crystalline, glass and metal foil in order of increasing resolving power and decreasing speed. Some of their characteristics are summarised in table IV.

4.1.1. Granular Screens

Granular screens are a mixture of small particles (5 to 15 μm) of a material which emits heavily ionising radiation promptly on neutron absorption, a luminescent material and a binding agent which should be transparent for maximum speed or slightly absorbent for best resolution. Stedman [10] has developed a screen which is a 1:2:1 mixture by weight of lithium-6 fluoride, zinc sulphide and perspex, giving a detection

TABLE IV Some characteristics of thermal neutron intensifying screens*

Screen	Thickness† mm	Average neutron detection efficiency‡ %	Tolerable beam γ-ray content§ roentgen/ neutron cm^{-2}	photons/ neutron	Inherent unsharpness¶ 10%–90% μm	slope μm
NE421 – granular	0.65	30	1.6×10^{-8}	27	1000	600
NE905 – glass	1.3	80	4×10^{-9}	6.6	600	300
Gadolinium foil	0.025	50	8×10^{-10}	1.3	70	70
Dysprosium foil	0.010	20	∞	∞	200	150

*All figures apply to use singly behind the film.
†These are the thicknesses of the screens selected for the work at Birmingham. With the exception of dysprosium they are approximately the maximum useful thicknesses.
‡Calculated as $\int_0^\infty \phi(E)\,\epsilon(E)\,dE / \int_0^\infty \phi(E)\,dE$, with $\phi(E)$ and $\epsilon(E)$ as given by Hawkesworth [11].
§Arbitrarily taken to be that which gives a gamma induced density of 10% of the neutron induced density. The tolerance for the gadolinium screen is doubled when a single emulsion film is used; that for dysprosium refers to the transfer technique.
¶See text for details.

efficiency of around 30% in a typical thermal neutron beam [11]. A development of this screen is marketed by Nuclear Enterprises (UK) Ltd of Edinburgh as NE421.

The basic nuclear reaction in a lithium-loaded screen is

$$^{6}Li + n \rightarrow {}^{3}H + {}^{4}He + 4.79 \text{ MeV}.$$

The tritons and alpha particles have considerable kinetic energy, some of which will be lost in the zinc sulphide particles which then emit light. Silver-activated zinc sulphide emits blue light (emission peak around 430 mμ) which provides a good spectral match with non-dye-sensitised photographic emulsions, and for maximum speed, films such as Kodak Royal Blue and Blue Brand, Ilford Industrial A and Polaroid Type 57 should be used in front of the screen. Representative characteristics of induced density versus thermal neutron exposure are given in fig. 12. It should be noted that these are not in general the same shape as those given by the manufacturers for radiations other than neutrons [11].

Zinc sulphide is relatively insensitive to gamma-radiation so that NE421 screens show good gamma rejection. However, resolution is poor, the edge unsharpness being around 1000 μm, and radiographs tending to be grainy. In so far as this is due to poor statistics, i.e. insufficient neutrons recorded before reaching the emulsion saturation density, it can be reduced by using a slower emulsion such as Ilford HP3.

Granular screens are generally used when the available beam intensity is low (with isotope and accelerator neutron sources and thick objects) and, as with all light-emitting screens, low-intensity reciprocity failure is observed. This means that in these cases a single characteristic (fig. 12) cannot give all the relevant information about necessary exposures. However, it has been shown at Birmingham that the Schwarzschild relation for calculating effective exposures is approximately followed for exposure times between 1 and 10^3 sec so that an available characteristic can be adjusted to suit the beam intensity. The Schwarzschild relation between radiation intensity I and exposure time t is that the effective exposure $= It^p$ for constant film density, where the Schwarzschild index p is a parameter of the emulsion and is usually around 0.74.

4.1.2. Glass Screens

Interest in glass converter screens arises from the need to improve the granularity and resolution of granular screen radiographs in situations where

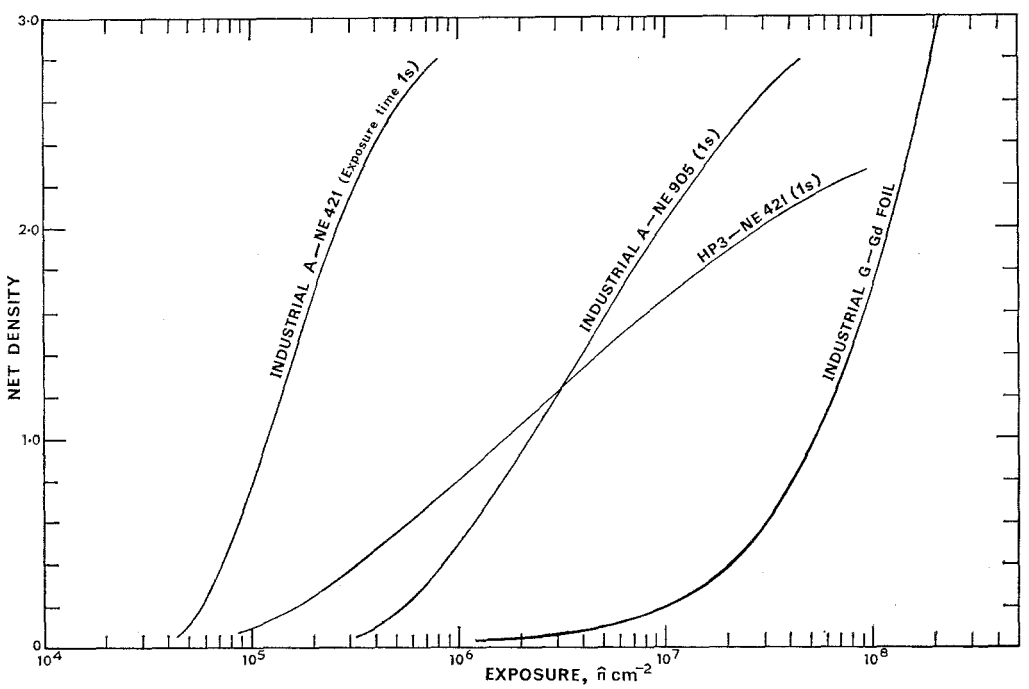

Figure 12 Typical neutron exposure characteristic curves for selected Ilford films in conjunction with granular (NE421), glass (NE905 – 1.3 mm) and foil (Gadolinium – 25 μm) neutron intensifying screens.

the beam intensity is not high enough for metal foil screens to be used. A suitable glass has been developed by Anderson *et al* [12] and is marketed by Nuclear Enterprises (UK) Ltd, as NE905. It is a silicate glass loaded with lithium-6 oxide and has cerium oxide as the scintillating agent. The peak emission is around 410 mμ so, again, the emulsions to use are those developed for tungstate screen X-ray work and Polaroid Type 57, the screen being placed behind the film unless the double screen technique is used.

Glass, 1.3 mm in thickness, gives images of good quality (edge unsharpness around 500 μm), and has a thermal neutron detection efficiency around 80% in a typical beam. However, cerium oxide is not an efficient scintillator and, as the characteristic curve (fig. 12) indicates, the speed is poor compared with that of granular screens, as is gamma rejection. Glass screens should, then, be used to obtain the highest resolution radiographs from accelerator neutron sources since they give better definition than granular screens and are rather faster than metal foil screens, which, though offering still better resolution, can only be used with accelerators of the highest yield.

4.1.3. Metal Foil Screens – Direct Exposure Technique

Many metals emit ionising radiation following neutron absorption and can thus be used as converter screens. The most useful is gadolinium [13] which has a very high absorption cross-section for thermal neutrons, the highest of all metals, coupled with the immediate emission of low-energy electrons from internal conversion of gamma-rays. The most prominent electron energy is 70 keV [14] which means that the range is short and the screen, therefore, has an inherently high resolving power (edge unsharpness $\sim$ 100 μm), particularly when used with thin emulsion films. Exposures to ionising radiation do not suffer from reciprocity failure but in spite of this, and the above advantages, gadolinium foil, the fastest metal converter screen, is slower than the light emitting screens. When gadolinium is enriched in gadolinium-157 (natural abundance 15.7%, absorption cross-section 240 000 barns), the speed will be similar to that of glass screens for long exposure times. The films to use are the fastest direct exposure X-ray films such as Kodak Kodirex and Ilford Industrial G, or electron microscopy films such as Kodak CF7 or perhaps Ilford HP3 for best resolution.

Gamma rejection is not very good, largely because long exposures are usually necessary and fast films have thick emulsions. The situation is improved when the high resolution films or single coated versions of Kodirex and Industrial G are used.

4.1.4. Metal Foil Screens – Transfer Exposure Technique

Perfect discrimination against gamma radiation can be obtained by employing the transfer technique. Most metals, unlike gadolinium, emit beta particles some time after neutron absorption, so, if such a metal is used alone as the detector, the radiographic image will be stored in the foil during the exposure. The screen may then be removed from the beam and pressed against a suitable film, such as Kodirex or Industrial G, in a cassette and the image will be transferred to the film as the foil activity decays.

The metal most suitable for the transfer technique is dysprosium which emits beta radiation with a maximum energy of 1.28 MeV and has a half-life of 2.3 h. The maximum useful screen thickness is 0.7 mm and nothing is gained by having either film or screen exposure greater than about 7 h. In practice, foils of thickness 0.1 to 0.25 mm are usually used as a compromise between speed and resolution. With reactor beams, which are required for sufficient intensity, screen exposures can be typically a few minutes and the films are usually exposed overnight. The screen thickness can be selected to give a speed similar to that with a gadolinium screen but the resolution is poorer, with edge unsharpnesses from 200 to 300 μm. The transfer technique is used for the radiography of radioactive materials, such as experimental rigs and structural materials from nuclear reactors and gamma ray sources, so that the need for a nuclear reactor beam is not usually inconvenient.

4.1.5. The Sensitivity of Photographic Image Recorders

Photographic recorders cover a wide range of sensitivities; exposure times required for some combinations of recorders and sources are given in table V.

The minimum thickness or change in thickness of an object, detectable by radiography, can be determined from the characteristic density-exposure curve of the recorder and the neutron cross-section of the object. A plot of induced density versus logarithmic exposure is usually

reasonably represented by a straight line with the slope (G) being known as the "contrast" of the recorder. Then the density $D = G(\log E - \log E_0)$* and the change in density produced by a small change in exposure is:

$$\Delta D = 0.434\, G\, \Delta E/E\,.$$

If this change is produced by a small change Δx in an object with macroscopic absorption cross-section Σ then:

$$\Delta D = 0.434\, G \Sigma\, \Delta x\,.$$

So the minimum detectable thickness ($\Delta x_{\min}$) in terms of the minimum detectable density change ($\Delta D_{\min}$) is:

$$\Delta x_{\min} = \frac{2.3\, \Delta D_{\min}}{G\Sigma}\,. \qquad (2)$$

In practice there is usually some background radiation (equivalent exposure B) which will reduce sensitivity. In the simplest situation B is independent of object thickness e.g. gamma background in the n-radiography of light or thin objects

$$\text{then} \quad C = \frac{\Delta x_{\min}}{x} = \frac{2.3\, \Delta D_{\min}}{G\Sigma x}\left(1 + \frac{B}{E}\right), \qquad (3)$$

where C is known as the "contrast sensitivity", it being usually more convenient to refer to the fractional thickness change detectable when background radiation cannot be neglected. (In equation 3 E is now the exposure from neutrons alone.)

The minimum detectable thickness of a material can be readily estimated with $\Delta D_{\min}$ at its usually accepted value of 0.02 and G from 1 to 3; for some photographic detectors G is even larger. When attenuation is entirely by absorption as in the case of n-radiography of cadmium objects, and there is little gamma background, the minimum thickness of cadmium detectable is approximately 1 μm. With organic materials, such as polythene, where beam attenuation is primarily by scattering, the minimum detectable thickness of approximately 50 μm, predicted by relation 2, must be increased by a factor of two or more, depending on the ratio of direct to scattered radiation at the detector [4].

4.2. Image Recorders for High Definition

It has been mentioned that photographic detectors using gadolinium converter screens are capable of giving high definition and, in fact, with typical objects, the divergence of a thermal neutron beam usually means that geometrical rather than screen factors control the attainable resolution. However, with extremely thin objects, (metallurgical samples are typical examples, figs. 2 and 7), where the screen is the limiting factor, the resolving power may be improved by using a very thin gadolinium screen and photographic emulsion [15]. As stated earlier, radioactive objects cannot be studied in this way.

A new technique capable of extremely high resolution and perfect gamma rejection is being developed [16] following the principles of neutron flux monitoring by the counting of fission fragment tracks in glass or mica [17]. More recently organic foils [16] have also been used. The fissile neutron converter screen is usually a foil of enriched uranium with a thickness around 5 μm, the range of the fission products. It may be convenient structurally to use thicker foils but the sensitivity will not be significantly increased. If the uranium foil is exposed to the neutron beam when pressed against a detector foil, any fission products stopped by the detector will, because of their heavy ionisation, cause damage along the length of their tracks. Regions of damage are preferentially attacked in chemical reactions so the detector foil may be "developed" by etching with hydrofluoric acid until the tracks are of the desired size. Berger and Kraska [16] use a cellulose nitrate film which is etched in a 6.5 N solution of sodium hydroxide, a more convenient technique than glass etched in hydrofluoric acid.

The main problem to date is one of printing the result to obtain a usable image, since photographic contact printing gives little contrast and photography with oblique lighting is not apparently practicable. The simplest way is to use a thin detector film which can be etched completely through to form a stencil. On printing, the density of ink dots per unit area will give a grey scale, and contrast and resolution will be controlled by the absorbency of the printing paper.

This new technique gives perfect discrimination against gamma rays, and Bhatt [17] has shown that with both phosphate glass and annealed mica the only source of background is spontaneous fission in the converter foil, which will be negligible during the time of a radio-

*When a foil screen is used the film exposure is to β-particles rather than light, there is then a linear relationship between density and exposure i.e. $D = GE$. Such a recorder is used as an illustration in the introduction.

graphic exposure. Consequently the technique is competitive with thin gadolinium foil-film detectors for high resolution applications, and with dysprosium foil-film detectors in the testing of radioactive objects. However, the neutron detection efficiency (tracks per incident neutron) will be only around 1% using a double screen system, to be compared with 50% for a single 25 μm gadolinium or 250 μm dysprosium screen. To attain comparable spatial resolution, a correspondingly larger exposure will be required and the stencil printing technique will not be used. When stencil printing is used, it is possible to enlarge the individual spots and therefore to give higher effective speeds at the expense of resolution so that it may prove to be the fastest "transfer" technique.

The spatial resolution attainable in the neutron radiography of stationary objects can be usefully thought of as composed of two terms; a geometrical term – due to the divergence of the neutron beam and the object-detector separation, and a detector term – due to the finite range of the radiation emitted by the screen. Following X-ray terminology these will be called "geometric unsharpness" U_g and "inherent unsharpness" U_i respectively.

For very thin objects placed on the detector, geometric unsharpness is virtually zero and the unsharpness inherent in the detector can be measured in the conventional way by examination of the images (fig. 13) of a knife-edge object, a clearly sheared gadolinium foil. The images formed by several screen-film combinations were scanned by a microdensitometer; representative traces are shown in fig. 14, and average unsharpness factors for each of the basic types of screen are given in table IV. The factors were measured on two criteria; the distance between the points where the maximum slope (projected) of the trace meets the lines of mean maximum and minimum density, and the distance between the 10 and 90% density points. These are only two of the several methods which might have been chosen [18], all of which are claimed to give values in reasonable agreement with subjective observations.

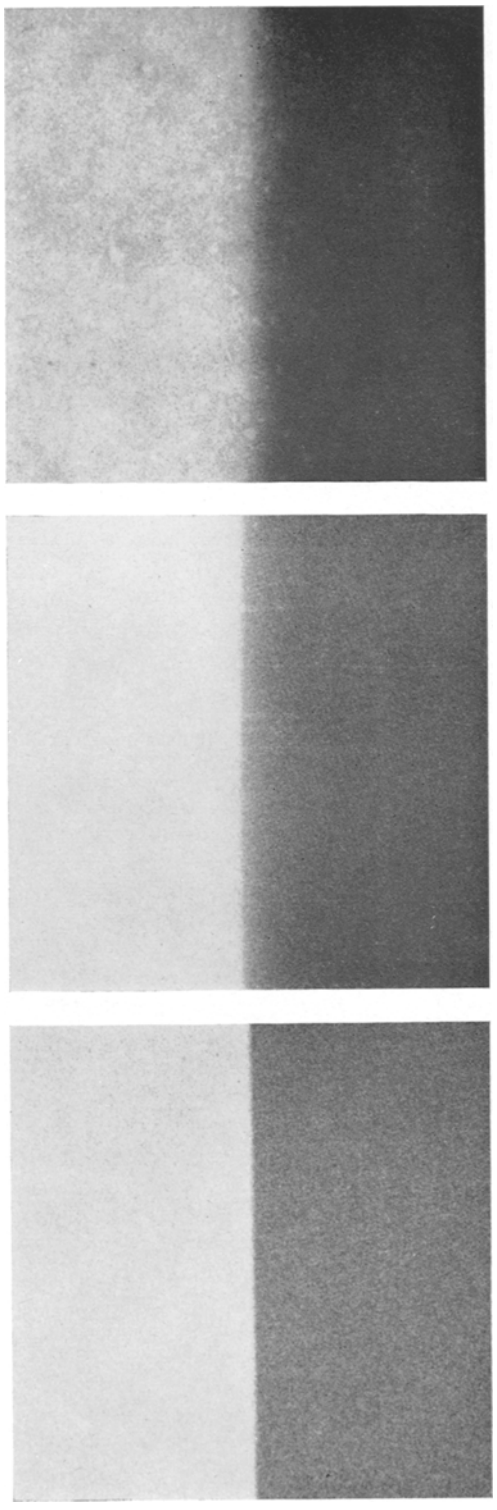

Figure 13 Images of a knife-edge (enlarged) showing the different image structure obtained with each of the three basic types of screen. The same film (Ilford HP3), processing conditions (Ilford PQX-1, 7 m) and printing paper (grade 2) were used in each case. Top: granular screen (standard NE421); middle: glass screen (NE905 – 1.3 mm); bottom: foil screen (gadolinium – 25 μm).

TABLE V Exposure times for a net photographic density of 0.5 with beams from each of the common classes of neutron source collimated to a divergence of 3° and 1°.

Detector screen	film	Nuclear reactor thermal flux 10^9n/cm² sec		Accelerator/Moderator thermal flux 10^7n/cm² sec		Isotope/Moderator thermal flux 10^5n/cm² sec	
		3° sec	1° sec	3° sec	1° sec	3° sec	1° sec
Granular	Ind. A	0.2	2	25	500	6000	—
Granular	HP3	1	10	250	5000	—	—
Glass	Ind. A	2	30	600	7000	—	—
Glass	HP3	15	260	5800	—	—	—
Gd foil	Ind. G	35	300	3500	32 000	—	—
Gd foil	Ind. B	100	800	8700	—	—	—

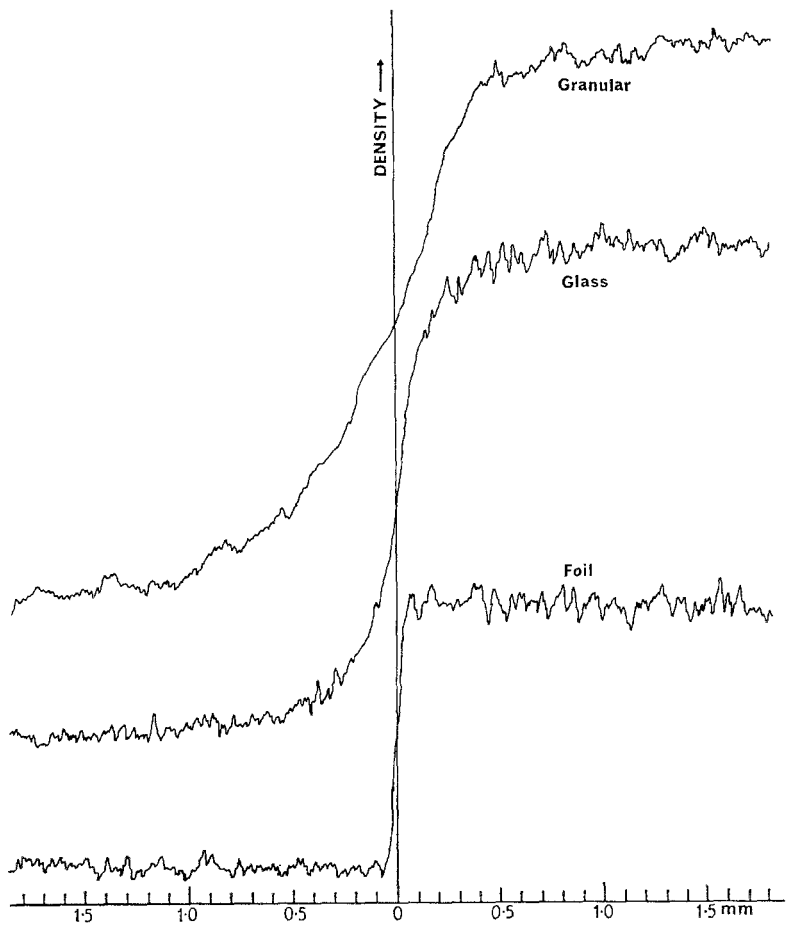

Figure 14 Typical microdensitometer traces across the image of a gadolinium knife-edge, for granular (NE421) and glass (NE905 – 1.3 mm) screens with Ilford HP3 film and a foil screen (Gadolinium – 25 μm) with Ilford Industrial B film. The density scale was 0.043/cm in all cases but since a suitable aperture was selected for each screen the granularity shown is not to scale.

The geometric unsharpness can be calculated from a knowledge of the divergence of the neutron beam and the distance between the relevant parts of the object and detector. It is usually taken as the width of the penumbra of the image, though when the variation of beam intensity with angle of divergence does not show a sharp cut-off, image assessment techniques, such as those described above, should be used.

To obtain an estimate of the size of the smallest

detail that will be detectable* on a radiograph of a specified object with a particular technique, the geometric and inherent unsharpness values must be combined to give a figure for the "total unsharpness" U_t which will be similar to the size of the minimum discernible detail. Klasens' suggestion [19] that $U_t = (U_g^3 + U_i^3)^{1/3}$ will be used by way of illustration, but again it is only one of several empirical methods that have been used. The metallurgical samples of fig. 7, about 3 mm in thickness, were radiographed using a beam with a divergence of 0.035 radians (2°) and a gadolinium screen. Thus $U_g \simeq 53$ μm (for detail at the centre of the object) and $U_i \simeq 70$ μm so that $U_t \simeq 80$ μm and the boron carbide particles of mean diameter 100 μm were expected to be seen individually; this was the case.

4.3. Electronic Image Recorders

The major disadvantage of detectors of the photographic type, the inability to give immediate image presentation, can be largely overcome by the use of Polaroid film. However, in certain applications, the ability to observe an image building up until it shows the relevant detail, to observe the movement of an object, or to inspect an object whilst it is being manipulated, may be of paramount interest. In such circumstances a range of electronic detectors may be considered.

An image intensifier tube can be used to observe the primary light-emitting neutron-converter screen with either direct or television presentation of the final image. Berger and his group are developing such a system, in conjunction with the Rauland Corporation of Chicago, using a lithium-6 fluoride/zinc sulphide neutron converter screen [20], and Spowart is working along similar lines at UKAEA, Dounreay [21]. Neutron detection efficiency is similar to that for the crystalline screens used with photographic films (20 to 40%) but, as the back of the screen is viewed rather than the front, resolving power will be poorer even when the finest intensifier tube is used.

An array of semiconductor detectors can be made by depositing the electrodes on the germanium or silicon in strips, those on one side of the detector being deposited at right-angles to those on the other [22]. For neutron applications such "checkerboard counters", along with other forms of position-sensitive semiconductor detectors, must be combined with a suitable converter screen. Neutron detection efficiency will be similar to that of the comparable photographic technique when the rear of the screen is viewed. A gadolinium screen may not be practicable because of the low energy of the electrons emitted and dysposium or a film of lithium-6 fluoride will probably be used. Visual presentation of the image will be expensive, particularly if high resolving power is required, but techniques to improve the contrast and resolution of the image may be applied directly; computer assessment of defects may be used also. Any detectors giving electrical impulses are particularly useful when an inspection technique is incorporated into an automatic process and for such applications the standard neutron detectors (BF_3 counters etc.) should not be overlooked. All these detectors are sensitive to gamma-radiation to a certain extent so it is unlikely that they will be usable for radioactive objects.

A neutron-sensitive visual spark chamber, providing complete discrimination against gamma radiation, has been described by Watts [23]. A layer of boron-10 was used for neutron conversion to give a detection efficiency of 5% for a typical thermal neutron beam. The electrode spacing limited the resolution to 1 mm in Watts' chamber for which photographic recording was used. Spatial resolution may be improved to perhaps 0.2 mm and electrical signals obtained from the chambers, or the sonic version, which can be used in the manner outlined for semiconductor counters.

5. Summary

This paper has discussed the particular advantages which neutrons have in radiographic applications and has provided information on sources and recorders available, and the techniques of using them. Examples of neutron radiographs have been referred to in the main text and more details on the experimental conditions are given in the legend to each radiograph.

Acknowledgement

The work on neutron radiography at Birmingham has received financial support from AERE, Harwell and we are grateful for it. We express our appreciation also to Mr R. S. Sharpe of the Non-Destructive Testing Centre, Harwell, for helpful discussion and to the Herald Reactor team, AWRE, for help with neutron exposures.

*This is an estimate of a dimension perpendicular to the neutron beam, as distinct from the smallest detectable change in thickness which was discussed earlier in connection with detector contrast.

References

1. J. THEWLIS, *Brit. J. Appl. Phys.* 7 (1956) 345.
2. *Idem*, "Progress in Nondestructive Testing", Vol. I, edited by E. G. Stanford and J. H. Fearon (Heywood, London, 1958) p. 113–119.
3. H. BERGER, "Neutron Radiography" (Elsevier Publishing Company, Amsterdam, London, New York, 1965).
4. J. P. BARTON, *Appl. Mats. Res.* **4** (1965) 90.
5. *Idem, Brit. J. Appl. Phys.* **16** (1965) 1.
6. J. P. BARTON and J. P. PERVES, *Brit. J. Non-Destr. Testing* **8** (4) (1966) 79.
7. K. H. BECKURTS and K. WIRTZ, "Neutron Physics" (Springer-Verlag, Berlin, 1964).
8. L. F. CURTISS, "Introduction to Neutron Physics" (Van Nostrand, New York, 1959).
9. J. WALKER, *Rep. Prog. Phys.* **30** (I) (1967) 285.
10. R. STEDMAN, *Rev. Sci. Instr.* **31** (1960) 1156.
11. M. R. HAWKESWORTH, *J. Sci. Instr.* **3** (1969) 235.
12. D. G. ANDERSON, J. DRACAS, and T. P. FLANAGAN, "Instruments and Measurements", Vol. II edited by H. Koch and G. Ljungberg (Academic Press, London, 1961) p. 616–630.
13. H. BERGER, *J. Appl. Phys.* **33** 1 (1962) 48.
14. L. V. GROSHEV, A. M. DEMIDOV, V. N. LUTSENKO, and V. I. PELEKHOV, "Atlas of γ-ray spectra from radiative capture of thermal neutrons" (Pergamon Press, London, 1959).
15. A. A. FAHMY, "Interaction of radiation with solids", edited by A. Bishay (Plenum Press, New York, 1967).
16. H. BERGER and I. R. KRASKA, *Trans. Amer. Nucl. Soc.* **10** 1 (1967) 72.
17. R. C. BHATT, Atomic Energy of Canada Ltd report AECL–2657 (1966).
18. R. HALMSHAW (ed) "Physics of industrial radiology" (Heywood Books, London, 1966).
19. H. A. KLASENS, *Philips Res. Rep.* **1** 4 (1946) 241.
20. H. BERGER, *Mater. Evaluation* **24** 9 (1966) 475.
21. I. C. HENDRY, *Nucl. Eng.* **13** 141 (1968) 106.
22. W. K. HOFKER, *Philips Tech. Rev.* **27** 12 (1966) 323.
23. H. V. WATTS, Armour Research Foundation report ARF 1164–27 1962).
24. W. C. REINIG, *Nuclear Applications* **5** (1968) 24.
25. The Radiochemical Centre, "Radioactive Products 1969–70" (UKAEA, Amersham, 1969).

Letters

Transmission Electron Microscopy of a Superplastic Alloy, Al-78 wt % Zn

New alloys have been developed which can be moulded as easily as plastics at high temperatures and yet are very strong at normal temperatures. Such crystalline materials, showing elongations of several hundred per cent [1] under certain conditions, are called "superplastic". Numerous materials which undergo phase transformations [2], as well as eutectic and eutectoid alloys, exhibit this phenomenon; the Al-78 wt % Zn alloy belongs to the latter class.

In a study of the Al-78 wt % Zn system, thin foils suitable for electron microscopy were prepared by using a Leitz ultramicrotome. Previous attempts to produce such thin foils by chemical etching or electrochemical thinning from the bulk were unsuccessful because of the different etching properties of the aluminium and zinc.

In this letter, transmission electron micrographs of Al-78 wt % Zn foils, prepared by ultramicrotomy, are described. The samples of the alloy in sheet form were pre-cut and mounted in gelatin capsules filled with Scotchcast* for support. Since the maximum area that can be cut with a diamond knife without knife damage is less than 0.5 mm^2, the capsules were dissolved in water after hardening of the Scotchcast, and the remaining block was shaped into a square pyramid with the sample strip located in the apex. The sections obtained were of uniform thickness ($\sim$ 2000 Å), and they formed a ribbon perpendicular to the knife edge on the surface of the water in the collecting trough. Because of the different electron absorption of aluminium and zinc, the contrast observed in the electron micrographs clearly indicates the type of phase present: regions appearing dark are rich in zinc, and light areas are rich in aluminium.

Fig. 1 shows a transmission electron micrograph of Al-78 wt % Zn which was heat-treated at 315° C and slowly cooled in air in an attempt to approach phase equilibrium. The typical pearlite structure with alternating layers of zinc and aluminium-rich phases is readily apparent. Electron microprobe analysis of a similar but

*Brand name, 3M Company.